Review of radio frequency microelectromechanical systems technology

S. Lucyszyn

Abstract: A review of radio frequency microelectromechanical systems (RF MEMS) technology, from the perspective of its enabling technologies (e.g. fabrication, RF micromachined components and actuation mechanisms) is presented. A unique roadmap is given that shows how enabling technologies, RF MEMS components, RF MEMS circuits and RF microsystems packaging are linked together; leading towards enhanced integrated subsystems. An overview of the associated fabrication technologies is given, in order to distinguish between the two distinct classes of RF microsystems' component technologies; non-MEMS micromachined and true MEMS. An extensive literature survey has been undertaken and key papers have been cited; from these, the motivations behind different RF MEMS technologies are highlighted. The importance of understanding the limitations for realising new and innovative ideas in RF MEMS is discussed. Finally, conclusions are drawn as to where future RF MEMS technology may lead. It is likely that the switch will continue to be the most important RF MEMS component, with future work investigating its enhanced functionality, subsystem integration and volume production. The focus of RF MEMS circuits will shift from the digital phase shifter to high-Q tuneable filters.

1 Introduction

While non-RF MEMS (radio frequency microelectromechanical systems) technologies are now established within high volume commercial markets, it is only now that RF MEMS technologies are becoming poised to step out of R&D laboratories and into commercial MEMS foundries. The first RF MEMS papers started to appear a quarter of a century ago; for example, within an IBM journal, a paper was published on electrostatically actuated cantilever-type capacitive membrane switches [1]. However, even though RF MEMS technology can still be considered to be in its infancy, a raft of interesting components and circuits has been demonstrated over the past 5-years [2]; the most notable are reviewed here, from the perspective of its enabling technologies.

It is useful to introduce RF MEMS by first defining common nomenclature. The term microsystems technology is generally used within Europe and it represents specific micromachined components (e.g. self-assembled or micromechanical), microelectromechanical systems (actuated using electrostatic, piezoelectric, magnetic or electrothermal mechanisms) and microfluidic technologies. In the US and Asia, the term MEMS (microelectromechanical systems, or structures) loosely represents microsystems technologies. In the context of MEMS, RF refers to radio frequencies beyond DC to sub-millimetre wavelengths. This distinguishes itself from optical MEMS technologies that encompass the mid-infrared to ultra-violet part of the frequency spectrum. With RF MEMS technology, lumped-element and distributed-element transmission line components are generally used. This does not, however, exclude the possibilities of implementing some of the quasi-optical techniques that are employed in optical MEMS.

A unique roadmap, showing the main RF MEMS technologies that are currently being reported in the open literature, worldwide, is shown in Fig. 1. The first important area to be considered is fabrication technologies, comprising predominantly either surface or bulk micromachining. These technologies are related to all other areas identified. For example, if only RF micromachined components are considered, surface micromachining has been used to realise 3-D planar inductors and transformers, self-assembled inductors and antennas and sliding planar backshort (SPB) impedance tuners; while bulk micromachining has been used to implement 3-D planar inductors and guided-wave structures (e.g. transmission lines, resonators, cavities and horn antennas). None of these micromachined components can be considered as true MEMS components, simply because there is no reconfigurable actuator involved in converting a control voltage or current into mechanical movement, once it has been manufactured. MEMS components are micromachined components, but not necessarily vice versa. Non-MEMS RF micromachined components have already, to some extent, been incorporated into RF MEMS circuits.

When considering a true RF MEMS component, in addition to the RF element, an electromechanical actuator is required; the most appropriate choice of which is very much dependent on the fabrication technologies available. By far, the most common actuation mechanism is electrostatic, followed by piezoelectric, magnetic and electrothermal. In addition to these generic forms, the scratch-drive actuator is becoming more popular. In principle, the scratch-drive can be based on some form of piezoelectric, magnetic or electrothermal actuation, although electrostatic actuation is most common.

IEE Proceedings online no. 20040405

doi:10.1049/ip-smt:20040405

Paper received 9th May 2003

The author is with the Optical and Semiconductor Devices Group, Department of Electrical and Electronic Engineering, Imperial College London, Exhibition Road, London SW7 2AZ, UK

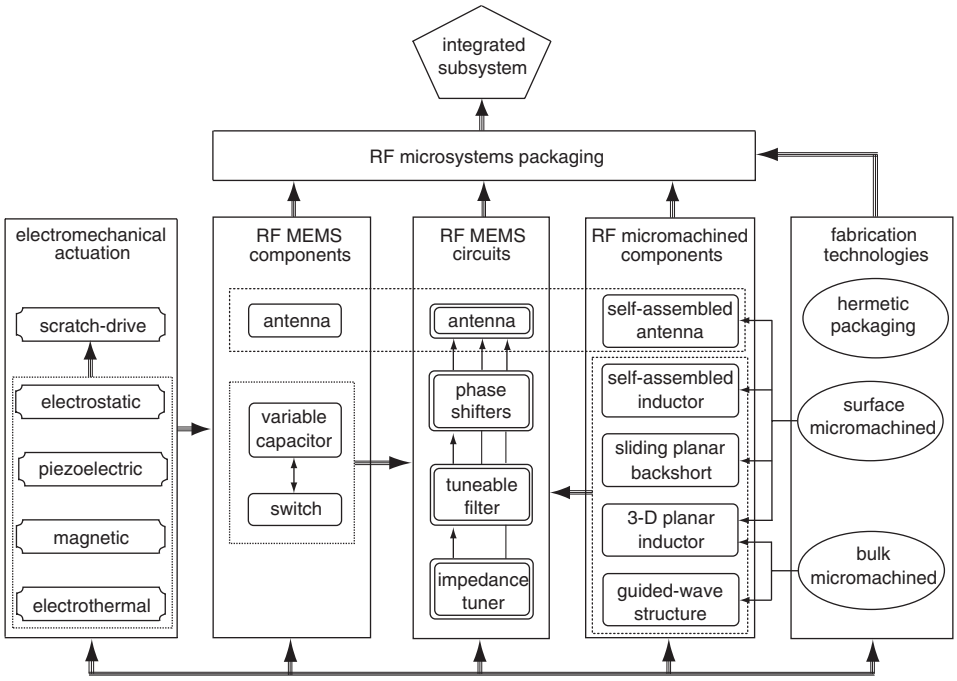

Fig. 1 *RF MEMS technology roadmap*

In terms of true RF MEMS components, there are only three generic types to have been reported so far: (i) the switch; (ii) the variable capacitor; and (iii) the antenna. By far, the single most important RF MEMS component is the switch. The reason for this is that it can be used to implement high performance and digitally-controlled components (e.g. *R*, *L* and *C* lumped-elements), circuits (e.g. attenuators, phase shifters, impedance tuners, filters and antennas) and subsystems (e.g. signal routing for implementing circuit redundancy, T/R modules and sectorised antenna arrays). While the RF MEMS switch offers a superiour performance over the PIN diode, the variable capacitor has the potential to supersede the simple varactor diode, especially in terms of tuning linearity and RF power handling. The RF MEMS variable capacitor can find applications in high-performance switches and analogue-controlled circuits (e.g. phase shifters, impedance tuners and filters). The only other generic RF MEMS component to be reported is the antenna, which has its radiating elements that physically move under some form of actuation mechanism.

With the main RF micromachined components, RF MEMS components and RF MEMS circuits being identified, it is now appropriate to link them all to the very important issue of RF microsystems packaging. With the appropriate choice of packaging solution, which is very much dependent on many external factors (e.g. RF performance, fabrication technologies and cost), RF MEMS components and circuits can be integrated into subsystems that can offer a significantly greater RF performance and enhanced functionality over conventional solutions.

2 Fabrication technologies

Before RF MEMS technologies are reviewed, the fabrication technologies used in their manufacture will first be introduced; an issue that is not so straightforward. This is because RF microsystems have evolved as a result of continual advances in a number of different manufacturing technologies that have merged together, leading to a blurring in their otherwise distinctive characteristic features. An attempt to provide a useful roadmap encompassing some of the main technologies is given in Table 1. Principally, these can be broadly partitioned into traditional multilayer and micromachining, which have both been applied to manufacturing of RF circuits since the 1970s.

2.1 Multilayer

As operating frequencies reduce, the size of both lumped-element and distributed-element components generally increase. As a result, chip sizes and therefore chip costs increase. While this is not such an important-issue for substrates used to realise hybrid microwave integrated circuits (HMICs) or multi-chip modules (MCMs), it is a very important driver when GaAs and more exotic semiconductors are used to realise monolithic microwave integrated circuits (MMICs). Multilayer technologies are used to increase package densities, by implementing traditional planar 2-D components with 3-D geometries [3].

With microfabrication technologies, a dielectric or metal layer is first deposited and then a photolithographic process is used to pattern the layer. This thin-film process is then repeated for the next layer, and so on. Since sub-micron feature sizes can be obtained, this technology is normally associated with monolithic circuits; for example, a 3-D millimetre-wave dielectric-filled metal-pipe rectangular waveguide [4]. In recent years, however, Japanese industry has been pioneering ways of increasing levels of integration. For example, NTT developed an ultra-compact 3-D passive circuit technology [5] and also its 'master-slice' technology [6]. With the former, 10 μm vertical gold walls and microwires have been constructed in air. With the master-slice technology, an upper ground plane covers selected areas of an MMIC's active layer. Passive circuits are then realised in a layer above this upper ground plane. This technique is then repeated so that a number of passive layers are stacked on top of one another. In the late 1980s, Plessey Research (Caswell), now Bookham Technology, and GEC-Plessey Semiconductors, now Intarsia Corporation, first started working together on multilayer processing for the development of 3-D multi-chip modules (MCM-D). Here, a number of aluminium layers, separated with thin

Table 1: Fabrication technology roadmap

	Manufacturing technology	RF components demonstrated	
		Non-MEMS	True-MEMS
Multilayer	microfabrication (etching of the dielectric layers; no sacrificial layers are used)	lumped-element components and 2-D and 3-D transmission lines (e.g. rectangular waveguides), master-slice and MCM-D (deposited)	
	substrate bonding (no etching of the substrate, other than for via holes)	MCM-L (laminated)	
Micromachining	surface (etching of the dielectric layers; sacrificial layers are used)	Inductors, rectangular waveguides, LIGA microstrip filters, and patch antennas	switches, variable capacitors, V-antennas
	bulk (etching of the substrate; etch-stop and sacrificial layers are used)	Membrane-supported transmission lines, rectangular waveguides, cavity resonator filters	
	wafer bonding (bulk-micromachined substrates are bonded together)	Microshield transmission lines, coupled-cavities, rectangular waveguide filters, horn antennas	variable capacitors

polyimide layers, are deposited onto either a silicon or sapphire substrate [7].

With substrate bonding techniques, high purity dielectric substrates are bonded together, using either solder-bump (i.e. flip-chip) technology, in order to create both electrical and thermal contacts between the substrates. Techniques have been developed by NTT for implementing 3-D HMICs, using a laminated-type of MCM process [8].

2.2 Micromachining

In essence, surface micromachining technology has evolved from multilayer microfabrication; the difference being that sacrificial layers are used. Here, micromachining is generally not applied to the substrate material, but on the dielectric and/or conductive layers above it. For example, the University of Bath reported a 600 GHz air-filled metal-pipe rectangular waveguide structure, realised using just a single wafer [9]. Here, a very thick layer of SU-8 photoresist was used to define the waveguide. After gold was deposited onto an SU-8 former, the sacrificial layer of SU-8 was removed to leave a 3-D metal structure.

Bulk micromachining generally uses selective crystallographic etching techniques of silicon wafer substrates [10]; exploiting differential etch rates between the crystallographic directions, due to the orientation of the silicon crystal planes, or undercutting etch resistant features. In addition to this, the Technical University of Darmstadt has been pioneering micromachined structures from III-V materials [11, 12]. Here, unlike with silicon, crystallographic etching techniques cannot be employed and so chemical etching is one alternative, but this is at the expense of poorer precision and profile definition.

In RF performance terms, the metal-pipe rectangular waveguide can be considered as the ultimate guided-wave structure, although package density is very poor indeed. The University of California first proposed the idea of implementing air-filled metal-pipe rectangular waveguides, using integrated circuit technology, back in 1980 [13]. More than a decade later, in collaboration with the University of Arizona, the California Institute of Technology demonstrated a W-band micromachined air-filled metal-pipe rectangular waveguide [14]. By using a two-wafer sandwich approach, they achieved a measured level of insertion loss of only 0.04 dB/λg at 100 GHz. Wafer-bonding continues to advance, with vertically integrated micromachined filters being demonstrated at frequencies as low as 10 GHz [15].

3 RF Micromachined components

Even though there are no reconfigurable electromechanical actuators incorporated, some consider 3-D waveguide, micromechanical and self-assembled structures to be MEMS components. Examples of RF micromachined guided-wave structures have already been cited in Section 2.2.

Lubecke *et al.* [16] reported a noteworthy example of a micromechanical RF micromachined component, by demonstrating a functional tuning element in a fully monolithic sub-millimetre-wave integrated circuit. Here, two micromechanical SPB impedance tuners were integrated with coplanar waveguide transmission lines, in a quasi-optical detector circuit operating at 620 GHz. The tuning elements were used to vary the power delivered to the detector over a range of 15 dB, by adding a variable reactance in series with an input antenna and a variable susceptance in parallel with the detector.

3.1 Self-assembled components

Within the past 3 years, a couple of self-assembled RF micromachined components have been reported; (i) the inductor; and (ii) the antenna. These components are not designed to be reconfigured, once manufactured, as true-MEMS components are; they are only designed to be erected out-of-plane only during the final stage of the manufacturing process. However, their importance to the future development of RF integrated circuits (RFICs) should not be overlooked.

Traditional planar spiral inductors lie on their host substrate and, as a result, suffer from unwanted effects. If the substrate is low cost (i.e. low resistivity) silicon, used in conventional RFIC technology, Q-factors can be very low indeed. For this reason, medium-to-high Q-factor resonators and filter circuits and low loss RF power combiners are located off-chip. Using micromachining, on-chip inductors can be integrated and spatially separated from the substrate, giving the following advantages:

1. Removing the substrate reduces parasitic capacitances and therefore increases the lowest self-resonant frequency, operating bandwidth and unloaded Q-factor. In addition, it removes the associated capacitive dielectric losses.
2. Removing the substrate reduces the energy coupled into the substrate and therefore the energy propagating as

surface waves and/or energy coupled into adjacent structures.

3. By increasing the distance between the inductor's current carrying windings and both the lossy substrate and nearby conducting layers (e.g. backside ground plane), induced eddy currents and therefore the associated energy lost through Joule's heating can be minimised.

4. With vertical inductors (i.e. those having their plane orthogonal to the surface of the substrate) more real-estate is available to increase the number or turns and/or conducting track width.

All these advantages increase the unloaded Q-factor of the inductor still further.

In practice, a number of techniques have been reported to spatially separate on-chip inductors from their substrate: (i) undercutting the substrate material from beneath the spiral [17]); (ii) locating the inductor on a platform, which is then raised above the substrate using scratch-drives [18]; and (iii) employing self-assembly [19–24]. With all these techniques, the lowest self-resonant frequency and unloaded Q-factor can be increased significantly, with almost no change to the value of inductance.

There are at least three methods of actuation that can be adopted, during the manufacturing process, to create a (near-) vertical inductor: (i) plastic deformation magnetic assembly (PDMA); (ii) tensile stress; and (iii) surface tension. With PDMA, permalloy (NiFe) strips are electroplated onto each hinged flap and an external DC magnetic field is applied to provide plastic deformation of the conducting hinges [19].

An example of a self-assembled patch antenna, employing PDMA, was also reported by the same team [25]. As the antennas is elevated out-of-plane, the operating frequency increases considerably, due to the capacitive loading of the substrate decreasing. Unfortunately, even though the radiation efficiency can be increased, due to the drop in energy radiating into the substrate, an extra 5 dB in loss results from absorption RF energy into the permalloy coating on the patch itself.

With the tensile stress approach, the inductor is patterned on polysilicon cantilevers, which are released from the substrate when the silicon oxide sacrificial layer is etched away [20]. This concept has been taken further by the Palo Alto Research Center; patterned molybdenum-chromium strips are sputter deposited with an engineered built-in stress gradient, so that when they are released from the substrate they curl up into a self-assembled solenoid inductor. Q-factors of up to 85 have been demonstrated at 1 GHz on standard CMOS silicon substrates [21].

The self-assembly approach developed at Imperial College London exploits the surface tension of solder hinges, to create the necessary lifting force [22–24]. Figure 2 shows a microphotograph of a three-turn spiral inductor, self-assembled using surface tension. The inductor, including air-bridge, was first fabricated in a similar way to conventional planar spiral inductors on the surface of the silicon wafer. The complete structure was then erected by applying the correct heating profile to melt the solder hinges.

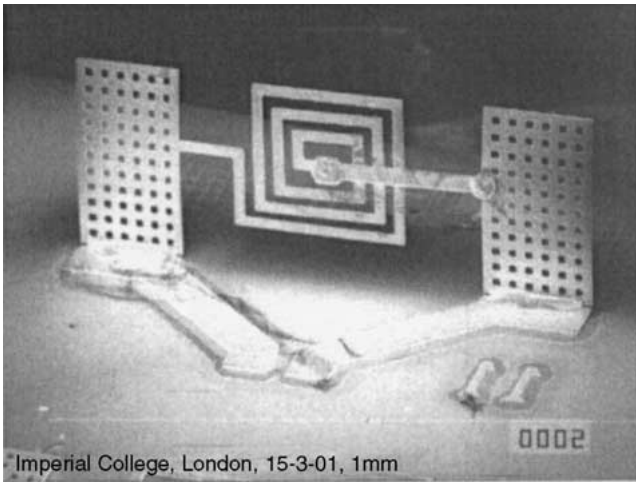

Fig. 2 *Multi-turn spiral inductor, self-assembled using surface tension [22–24]*
Reproduced by permission of G. W. Dahlmann and E. M. Yeatman

4 Electromechanical actuation

With RF MEMS components and circuits, there could be many conflicting requirements that need to be considered early on in the design process. For example:

1. intrinsic RF performance (e.g. insertion loss, isolation and return losses);

2. actuation mechanism (e.g. electrostatic, piezoelectric, magnetic and electrothermal);

3. control parameters (e.g. voltage, current, power, residual energy and speed);

4. fabrication technologies (surface and bulk machining, wafer bonding and hermetic packaging);

5. layout (e.g. area, topology and topography);

6. packaging (e.g. standardisation and extrinsic parasitics effect on overall RF performance);

7. subsystems integration (e.g. self-actuation and cost).

While RF MEMS technology can offer unprecedented levels of intrinsic RF performance, a significant limitation in any one of the above requirements can mean the success or failure in its implementation. For this reason, RF MEMS components and circuits are subjected to very severe practical trade-offs in their designs [26]. Indeed, while many initial designs may seem appropriate, it is not until all the above requirements have been carefully considered that a much smaller number of candidate solutions remain for detailed CAD simulation (i.e. using electromagnetic, circuit, mechanical and thermal simulators).

In practice, once the intrinsic level of RF performance of the MEMS component or circuit has been decided, appropriate methods of actuation can be investigated. Electrostatic actuation is, by far, the most common, as it can produce small components that are robust and relatively simple to fabricate. They are also relatively fast and tolerant to environmental changes. In principle they consume almost no control power; and only when switching between states, although some residual energy is required to hold them in the actuated state. The main disadvantage with electrostatic actuation is that it is difficult to combine a low actuation voltage with good switch isolation, because of small spatial separation distances between electrodes. Moreover, self-actuation by the RF signal being switched can be a serious problem.

Piezoelectric actuation is typically based on a bimorph cantilever or membrane, where a differential contraction due to the piezoelectric effect causes the structure to bend. Here, fast actuation speeds can be obtained. Unfortunately,

there is usually also a differential thermal expansion of different layers that causes parasitic thermal actuation. In order to avoid this, the structure has to be designed to be symmetrical with respect to the thermal characteristics of the layers. Integrating piezoelectric materials into a MEMS environment is also very problematic, because films are difficult to pattern and the processing involves high crystallisation temperatures.

Both magnetic and electrothermal actuation offer the advantages of low control voltages and high contact force. However, unlike their electrostatic and piezoelectric counterparts, they are slow, draw a relatively high current and dissipate significant levels of power when held in the actuated state. Also, magnetic actuators tend to be relatively large and difficult to fabricate, because they require a 3-D coil with a soft-magnetic core.

5 RF MEMS components

The enabling technologies (i.e. fabrication, RF micromachined components and actuation mechanisms) that are needed to implement RF MEMS components have been reviewed. However, before practical demonstrators can be cited, it is important to understand the key requirements for each component.

5.1 Switches

For the past few decades, RF integrated circuit switching has been performed by PIN diodes within HMICs and cold-FETs within RFIC/MMICs. The former can deliver a superiour RF performance. For example, M/A-COM's MA4AGSW1 AlGaAs SPST reflective PIN diode switch can achieve a measured: ON state insertion loss of less than 0.4 dB, from DC to 50 GHz; OFF state isolation better than 45 dB, from 18 to 50 GHz; and input and output return losses better than 15 dB, from DC to 50 GHz. The latter is the result of the inherent compatibility with active-FET processing, but the performance is much worse than that obtained with PIN diodes. With both PIN diodes and cold-FETs, intermodulation distortion presents serious limitations at higher RF-power levels, however, general PIN diode performance is still formidable.

Systems' architectures can be greatly enhanced, in terms of greater performance and functionality and reduced complexity and cost, if switch performance can be improved even further with the use of RF MEMS technology [26, 27]. The RF performance of a switch can be represented by the following cut-off frequency figure-of-merit:

$$f_c = \frac{1}{2\pi R_{on} C_{off}} \tag{1}$$

where R_{on} is the ON state resistance, effectively representing the ON state insertion loss, and C_{off} is the OFF state capacitance, effectively representing the OFF state isolation

Goldsmith *et al.* [28] reported RF MEMS switches with an extracted $f_c = 2$ THz, back in 1995; which represents at least a two orders of magnitude improvement over that attainable with PIN diodes.

There are two generic types of RF MEMS switch: (i) the ohmic contact (metal-air-metal, MAM); and (ii) the capacitive membrane (metal-insulator-metal, MIM). The main advantages of the former are that a very low ON state insertion loss and very high OFF state isolation can be achieved. The reason for this is that the ohmic contact area needed for this type of switch can be very small indeed. This small area therefore creates a small parasitic capacitance when the electrodes are separated and, thus, good isolation can be achieved. Unfortunately, ohmic contact switches are highly susceptible to corrosion, stiction and microscopic bonding of the contact electrodes' metal surfaces. Moreover, considerable force is required to create a good metal-to-metal contact and this may not be possible under certain types of actuation.

With the capacitive membrane switch, a trade-off has to be made; increasing the electrode surface area improves the ON state insertion loss, but compromises the OFF state isolation. As a result, electrode separation needs to be maximised and this may not be possible with certain actuation mechanisms. The main advantage of the capacitive membrane switch is the longer lifetime. The lifetime of an ohmic contact switch is typically several orders of magnitude less than that of a capacitive membrane switch. Another advantage of the capacitive membrane switch is that the ON state insertion loss is independent of the contact force, which relaxes the requirement of the actuation mechanism.

Nearly all RF MEMS switches are based on an out-of-plane electrostatically actuated suspension bridge- or cantilever-type, as illustrated in Fig. 3*a*. The condition of snap-down (or pull-down or pull-in) occurs when the electrode separation decreases below two-thirds of the fully open condition. As a result, it is important to be able to calculate the approximate actuation voltage, V_S, at which snap-down occurs. Snap-down occurs at the point where the electrostatic attractive (downward) force is equal to the linear restoring (upward) spring force. It can be show, from simple beam theory (i.e. $t \ll W \ll L$) that:

$$V_S \cong \sqrt{\frac{8kh_{up}^3}{27\varepsilon_o A}} \begin{cases} \sqrt{\dfrac{128Et^3h_{up}^3}{27\varepsilon_o L^4}} & \text{for a suspension bridge} \\ \sqrt{\dfrac{2Et^3h_{up}^3}{27\varepsilon_o L^4}} & \text{for a cantilever} \end{cases} \tag{2}$$

where k is the effective spring constant h_{up} is the electrode separation when the beam is in the 'up' position, ε_0 is the permittivity of vacuum, E is Young's modulus for the beam material, A is the pull-down electrode area ($\sim LW$), L is the beam length, W is the beam width, and t is the beam thickness.

Clearly, the cantilever offers the important advantage of a factor of eight reduction in the actuation voltage, when compared to that required by the suspension bridge. In practice, decreasing k decreases the actuation voltage but increases the switching time and, hence, a trade-off exists between the actuation voltage and speed. A low effective spring constant also causes an increased sensitivity to microphonics. Practical considerations set a lower limit to the actuation voltage, such as self-actuation and stiction. With a switch designed so that the RF signal is superimposed onto the control voltage, self-actuation can occur.

In practice, the actuation voltage for simple suspension bridge designs is too high for many applications and so meandering can be introduced to lower the effective spring constant. Pacheco *et al.* [29] demonstrated a 9 V electrostatically actuated switch, having a five-meander arm at each of the four corners of the capacitive membrane bridge. Here, the capacitance ratio = 2.5 pF/47 fF = 43; insertion loss = 0.16 dB at 40 GHz; isolation = 26 dB at 40 GHz; and self-actuation occurs with a mean RF power of 6.6 W. A microphotograph of a similar switch is shown in Fig. 4, the corresponding actuation voltage against number of meanders is listed in Table 2.

Failure due to stiction can occur when the stiction force is greater than the restoring force of the spring in the 'down'

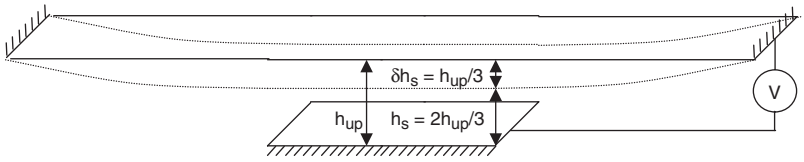

Fig. 3 *Suspension bridge under electrostatic actuation*
Note that δh_s is the beam deflection at snap-down and h_s is the electrode separation at snap-down

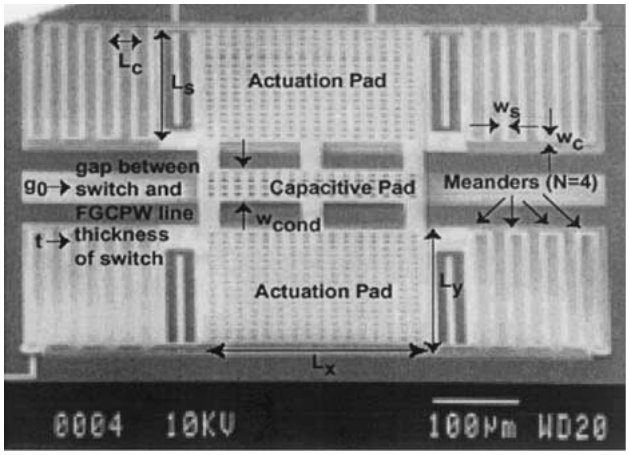

Fig. 4 *Capacitive membrane switch, designed and fabricated at The University of Michigan at Ann Arbor [29]*
Reproduced by permission of IEEE

Table 2: The actuation voltage as a function of the number of Meanders [29]

Number of meanders	Designed V_s V	Measured V_s, V
1	3.90	35
2	2.75	28
3	2.24	20
4	1.94	15
5	1.74	9

position. It is difficult to predict the stiction force, as this depends on the surface quality of the electrodes as well as on the environmental conditions (i.e. humidity and surface contamination of the electrodes). With low actuation voltage switches, like the one in Fig. 4, stiction can be a serious problem. For this reason, reliability and hermetic packaging issues are now of the highest priority amongst potential manufacturers [27].

An example of high isolation W-band RF MEMS switches was reported by Rizk *et al.* [30], employing electrostatically actuated capacitive membrane bridge-type structures. Here, a T-match design resulted in an ON state insertion loss of <0.9 dB and an OFF state isolation of >18 dB, across the 75 to 110 GHz frequency range. With a π-circuit design, an ON state insertion loss of <1.2 dB and an OFF state isolation of >30 dB was achieved across the 75 to 110 GHz frequency range.

In addition to electrostatically actuated switches, RF MEMS technology has been used to implement magnetically actuated and electrothermally actuated switches. With the former, a micromachined magnetic latching switch has been demonstrated by Ruan *et al.* [31] operating from DC to 20 GHz and with a worst-case insertion loss of 1.25 dB and an isolation of 46 dB. The device is based on preferential magnetisation of a permalloy cantilever in a permanent external magnetic field. A short current pulse, through an integrated coil underneath the cantilever, achieved switching between two stable states. With an actuation voltage <5 V and resistance relay of ~ 100 mΩ, the switching energy <100 µJ.

Blondy *et al.* [32] demonstrated an electrothermally actuated millimetre-wave RF MEMS switch. The switch is constructed using a stress-controlled dielectric bridge, which buckles when heated. Here, resistors are fabricated into both beam supports. When a 5 V bias is applied to the switch, the resistors heat up and the beam buckles, thus, closing the switch. The insertion loss has been estimated to be 0.2 dB at 35 GHz and the turn ON and turn OFF times were measured to be 300 µs and 50 µs, respectively.

5.2 Variable capacitors

Variable capacitors are invaluable for implementing phase shifters and providing frequency control of tuners, filters and antennas. For these applications, maximising the capacitor's Q-factor is of paramount importance, for minimising loss and maximising noise performance. Until recently, only varactor diodes could provide voltage control of capacitance. However, while these devices are useful for frequency agile applications, they can exhibit relatively low Q-factors, are sensitive to even medium RF power levels and generally do not exhibit linear frequency tuning characteristics.

RF MEMS capacitors can overcome some, if not all, of the disadvantages of varactor diodes, but this is at the expense of much slower control speeds. In principle, the switch is a special case of a variable capacitor. As a result, the variable capacitor is commonly implemented with a switch-type of design; replacing digital with analogue control voltages. With an electrostatically actuated switch, snap-down severely limits the available tuning range, however, even this problem can be minimised or eliminated with the use of a passive series feedback capacitance to remove this instability [33].

An interesting example of how variable capacitors can be implemented in MEMS technology was reported by Chiao *et al.* [34]. With one design, a parallel-plate variable capacitor was constructed by fixing the lower plate onto the substrate and a raised platform acted as the upper plate. Here, two scratch-drive actuators located at opposite sides of the capacitor either pulled or pushed the support arms of the platform; hinges translated the lateral movement of the microactuators into vertical movement, in order to vary the gap spacing between the two metal plates. With this approach, a 2×2 mm^2 parallel-plate capacitor was realised. The gap spacing can be varied between 1 and 100 µm, in increments of 20 nm. Preliminary results found a maximum capacitance of 35 pF and a minimum capacitance of 0.5 pF. The breakdown voltage was found to be >200V, which is much greater than that for varactor diodes.

Another type of surface machined variable capacitor was also reported by Chiao *et al.* [34]. Since linearity of tuning can sometimes be more importance than dynamic range, circular parallel-plate variable capacitors were realised. The top plate, which is electrically isolated from the fixed bottom plate, is physically attached to two circular scratch-drive actuators. These actuators move in opposite directions (i.e. either in a clockwise or counter-clockwise direction), which allows the top plate to rotate by $\pm 90^{\circ}$. The gap between the plates is 2 μm and the overlapping area can be varied by an amount corresponding to a 0.5° increment in angular rotation.

Rockwell Science Center demonstrated a bulk machined electrostatically actuated RF MEMS variable capacitor, having interdigitated fingers [35]. Here, high aspect ratio single-crystal silicon was micromachined using 25 μm deep reactive ion etching, as shown in Fig. 5. This capacitor offers high tuning linearity, a small part count (making it less prone to failure) and is small in size. At a tuning voltage of 5.3 V, the maximum capacitance was 6 pF, with a 4:1 capacitance-tuning ratio, and the unloaded Q-factor was 265 at 500 MHz [35]. Finally, the development of electro-thermally actuated RF MEMS variable capacitors was reported by Feng *et al.* [36].

5.3 Antennas

Integrating a micromachined antenna with RF MEMS switches or variable capacitors, to provide some form of frequency tuning, is not difficult. However, to implement steerable antennas in true MEMS technology is notoriously problematic, for at least two important reasons: firstly, if the radiating elements are detached from the supporting substrate, it cannot exploit the size reducing attribute of the dielectric. Secondly, antennas are very sensitive to the presence of adjacent structures and feed line discontinuities. As a result, actuation mechanisms can easily interact with the antenna to distort the desired radiation pattern.

A true RF MEMS reconfigurable Vee antenna has been reported [37]. This planar antenna can have its far-field radiation pattern electrically altered using microactuators. An illustration of the 17.5 GHz antenna is shown in Fig. 6, employing a three layer polysilicon surface micromachining process. Here, the arms of the Vee antenna, used to form the radiating aperture, are moved using linear scratch drive actuators. The ends of these arms are hinged to anchors. Lateral movement of the actuators (20 nm per 70 V biasing pulse) is translated to rotational movement of the arms, by the use of moveable hinges that are not anchored to the substrate. Each antenna arm is capable of independent movement, giving the possibility of far-field radiation beam-steering and also beam-shaping. The directivity for the

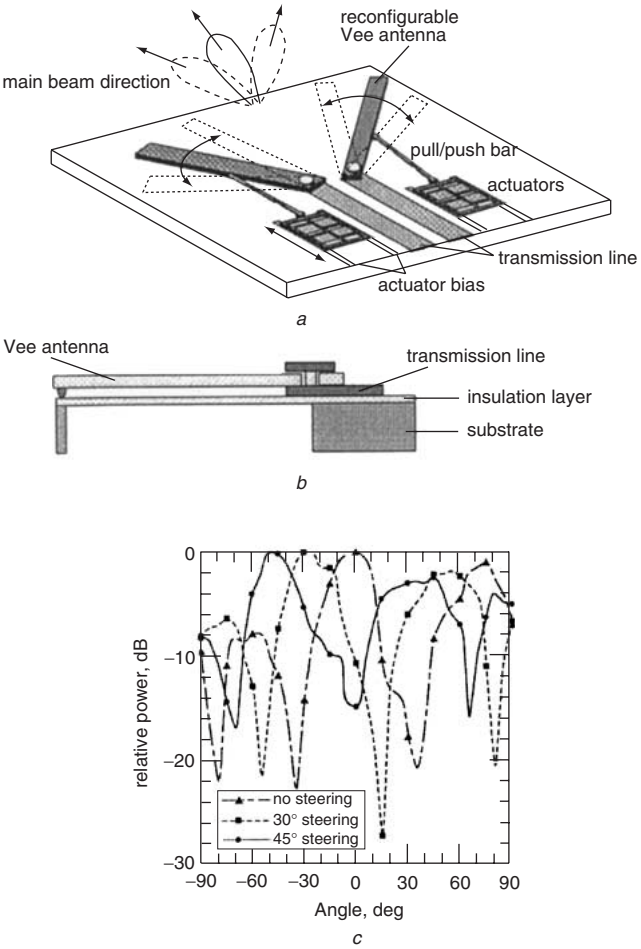

Fig. 6 *Reconfigurable Vee antenna [37]*
a Isometric view
b Side view
c Measured beam steenng performance
Reproduced by permission of IEEE

antenna was estimated (from measured 3 dB beamwidths) to be about 38, while cross-polarisation levels of below 20 dB were also reported. With a fixed Vee angle of 75°, the arms were rotated to 30° and 45° off-boresight, demonstrating beam steering, as shown in Fig. 6*c*. The design was further enhanced by the use of a true MEMS SPB impedance tuner [34].

Another example of a true RF MEMS antenna was reported by Baek *et al.*, demonstrating 2-D beam steering under magnetic actuation [38]. Here, an array of four 60 GHz patch antennas was arranged on a benzocyclobutene (BCB) substrate, having two degrees of freedom with

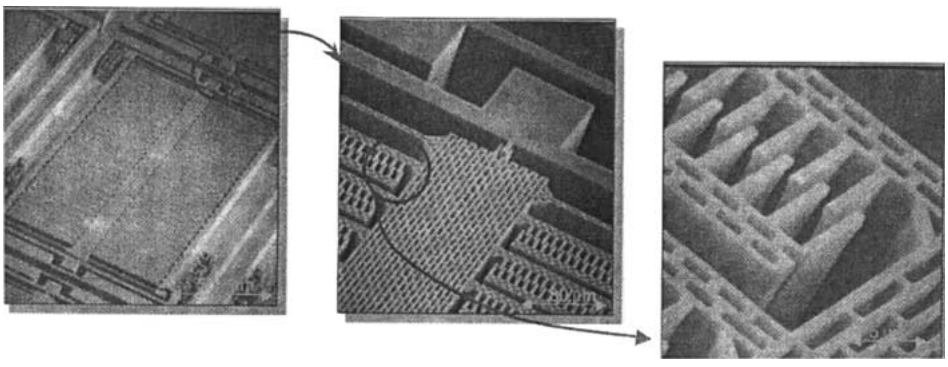

Fig. 5 *Electrostatically actuated bulk-micromachined silicon variable capacitor, designed and fabricated at Rockwell Science Center [35]*
Reproduced by permission of IEEE

the aid of orthogonal BCB torsion bars attached to BCB frames. A scan angle of $\pm 20^{\circ}$ was achieved.

6 RF MEMS circuits and subsystems

6.1 Phase shifters

A phase shifter is a control circuit found in many microwave communication, radar and measurement systems. Historically, one of the main reasons why conventional MMIC technology came about was because of the need to miniaturise phase shifters so that they could be easily integrated into compact phased antenna arrays. In principle, phase shifters could be placed directly between the antennas' radiating elements and their associated T/R modules, to create a fully distributed 2-D phased array antenna system. The holy grail of phase shifter designers has been to realise a 4-bit digital phase shifter having a sub−1 dB worst-case level of insertion loss. The reasons for attaining such performance would be to relax both a transmitter's power amplifier and a receiver's low noise amplifier specifications, thus, helping to dramatically reduce the cost of future front-end microwave subsystems. For phased array applications, low DC control power and repeatable batch processing are also important goals.

There are many different topologies that can be used to implement a digital phase shifter or true time delay network [3]: switched-line (having one or more cascaded stages of switched delay lines, with two switches per stage; reflection topology (having a one or more cascaded directional couplers, reflection terminations with either lumped- or distributed-elements and single-pole multiple-throw switches); loaded-line (periodically loaded with capacitive membrane SPST switches); and switched-filter; (having cascaded stages of low-pass and high-pass filters that are switched-in using either two SPDT switches per stage or a DPDT switch between stages).

The past 5 years have seen a flurry of papers on RF MEMS digital delay lines. Pillians *et al.* [39] reported a 4-bit monolithic switched-line delay line with microstrip on high-resistivity silicon. Here, MEMS capacitive membrane switches were employed, with $C_{ON}/C_{OFF} \sim 100$ and an actuation voltage of 45 V. The 5% fractional bandwidth was due to the extensive use of resonant stubs; however, at 34 GHz the insertion loss was low at 2.5 dB and the return loss was >15 dB. In the past couple of years, a team from the Rockwell Science Center have demonstrated high performance DC to 40 GHz 3-bit and 4-bit true time delay networks, using SPDT switches, on GaAs [40, 41]. Figure 7 shows the measured performance of this state-of-the-art RF MEMS phase shifter. Most recently, Tan *et al.* [42] demonstrated a similar performances with their DC to 20 GHz 2-bit and 4-bit true time delay networks, using SP4T switches, on GaAs.

Malczewski *et al.* [43] also reported a two-stage 2-bit reflection-type delay line, with tapped delay line reflection terminations. The same transmission line medium, substrate and MEMS switches were used as with the earlier switched-line example [39]. At X-band, the measured insertion loss was around 1.5 dB, with 60% of this loss being attributed to the Lange directional couplers.

MEMS distributed loaded-lines have also been reported. By applying a single bias voltage to either the signal conductor of the CPW line or the MEMS bridges lying over this centre conductor, the effective distributed capacitance of the line can be changed, which in turn changes the phase velocity and, thus, the associated propagation delay through the transmission line. Using this principle, Borgioli *et al.* [44] reported a 1-bit ultra-wide bandwidth distributed loaded-line. Again, MEMS capacitive membrane switches were employed, with $C_{ON}/C_{OFF} \sim 7.5$ and having an actuation voltage of 75 V. Here, an 8.6 mm long CPW line on a glass substrate achieved a DC to 35 GHz bandwidth, with a relative phase shift and insertion loss of 270° and 1.7 dB, respectively, at 35 GHz. Because of the variation in the characteristic impedance of the CPW line, from 66 Ω in the OFF state to 38 Ω in the ON state, the inherent impedance mismatching creates unwanted ripples in all the frequency responses. The same team then went on to report a 3-bit distributed loaded-line using the same transmission line medium, substrate and MEMS switches [45]. Using the same topology and almost identical MEMS technology as UCSB, Hayden and Rebeiz [46] went on to report a 1-bit X-band distributed loaded-line that achieved a relative phase shift of 270° at 10 GHz. The OFF and ON state insertion losses were 0.48 and 0.72 dB, respectively. The same team went on to demonstrate a 2-bit implementation at X-band [47]. Over the past couple of years, MAM capacitors have replaced MIM switches; with Kim *et al.* [48] demonstrating a 4-bit 40 to 70 GHz implementation and later Hayden and Rebeiz [49] reported a DC to 37 GHz version.

For a 4-bit switched-line delay line, a number of relatively long reference transmission lines are required at microwave frequencies. The main drawback with conventional monolithic technology is that insertion loss may vary considerably between states. This limitation can be minimised by utilising low loss micromachined lines. For example, micromachined thin-film microstrip could be used and this is ideal for meandering, thus minimising the size of the circuit. Here, suitable micromachining techniques need to be developed in order to provide the low transmission losses and be integrated with low loss/high isolation SPDT switches. Moreover, if membrane supported CPW lines are employed, great care must be made to avoid unwanted modeing, since insertion phase can be very sensitive to multi-modeing.

Similar techniques recommended for the switched-line delay line can also be associated with the reflection-type delay line; however, a low loss 3 dB quadrature directional coupler is needed. This would be possible with a micromachined multilayer broadside coupler. To date, no reflection-type digital delay line has been reported that combines micromachined coupled lines with MEMS switches.

For a 4-bit implementation of the distributed loaded-line, line lengths become excessive. Moreover, even meandered transmission lines would require considerable chip space, while meandering of loaded-CPW lines is not recommended. Also, the inherently poor return loss performance may result in unacceptable ripples in the insertion loss, which are then translated to ripples in the insertion phase, relative phase shift and group delay frequency responses. For these reasons, this type of delay line is expected to be the least likely to meet the demanding electrical specifications of future high performance applications.

6.2 Impedance tuners and filters

Chiao *et al.* [34] reported a planar impedance tuner in coplanar stripline technology, as shown in Fig. 8. Here, a SPB on top of the planar transmission line forms a moveable short circuit. It allows for variations in the length of short circuit transmission line stubs, using scratch-drive actuators. This idea is an extension of the micromechanical SPB impedance tuner demonstrated by Lubecke *et al.* [16].

The most common form of RF MEMS tuning arrangement is to employ either surface micromachined switches or

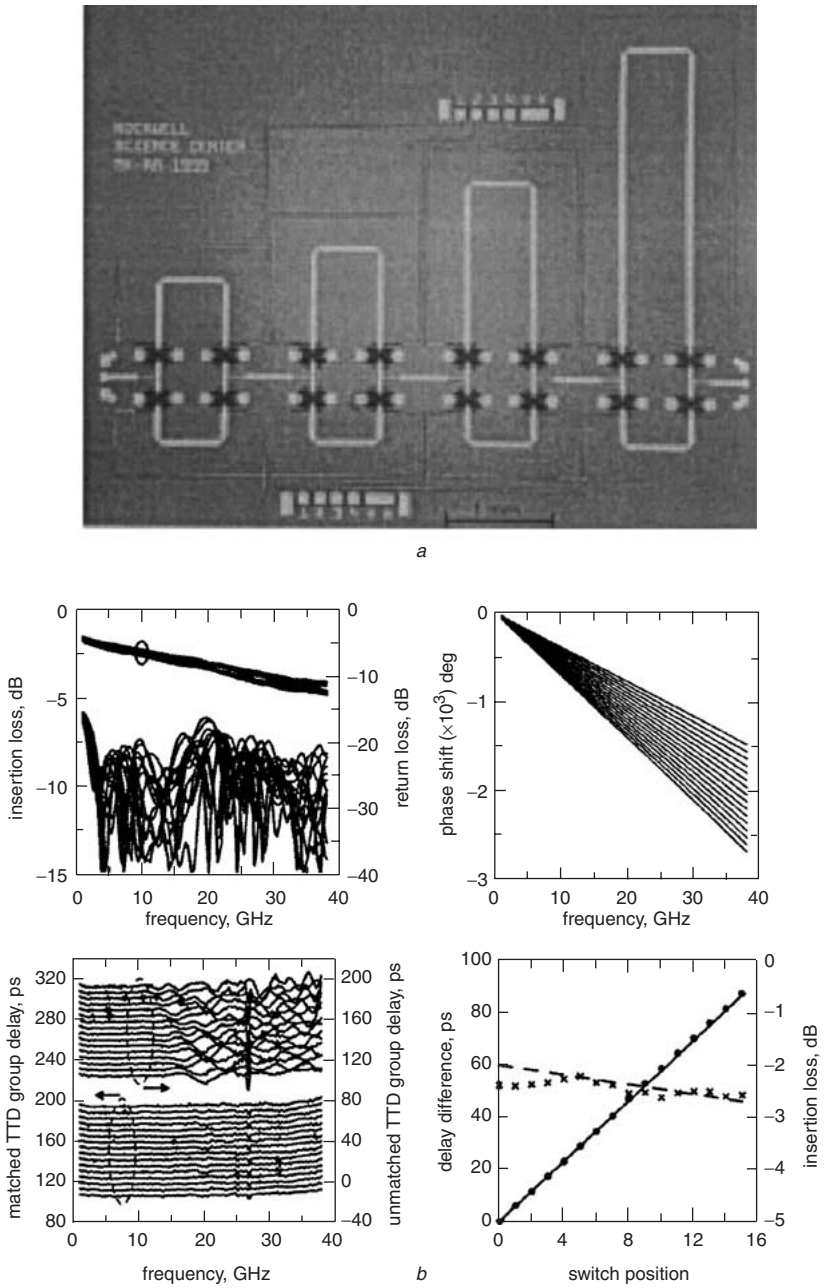

Fig. 7 *DC to 40 GHz 4-bit true time delay network on GaAs [40, 41]*
a Microphotograph
b Measured performance
Reproduced by permission of IEEE

variable capacitors. Kim *et al.* [50] and Papapolymerou *et al.* [51] have demonstrated a range of different RF MEMS tuners using such methods. Bulk machined RF MEMS variable capacitors have also been employed in high-Q micromachined *L–C* tank circuits (intended for on-chip voltage-controlled oscillators) [52], and hybrid assembled filter circuits [35].

Like phase shifters, filters having <1 dB pass-band insertion loss can replace SAW filters in GPS and mobile phone handsets. Low loss RF MEMS filters could enable the LNA to be placed after the filter and, thus, avoid any saturation due to out-of-band noise contributions. Kim *et al.* [53] demonstrated two-pole lumped-element and distributed-element tuneable band pass filters, centred at 26 GHz and 30 GHz, respectively. Here, surface micromachined cantilever-type variable capacitors were employed, having electrode separations 6 μm down to 4 μm under electrostatic actuation. The minimum levels of pass band insertion loss were 4.9 dB and 3.8 dB, respectively. The same team then went on to report similar techniques at 50 GHz and 65 GHz [54]. The 65 GHz filter had a tuning bandwidth of 10% and an insertion loss of 3.3 dB.

An interesting distributed-element RF MEMS filter was simulated by Mercier *et al.* [55]; tuneable resonators can be formed by sections of CPW line that are periodically loaded with electrostatically actuated bridge-type variable capacitors. A two-pole filter was simulated at 39 GHz using this technique. With the electrode separation varying from 1.8 μm down to 1.2 μm, the center frequency could be tuned from 40.4 GHz down to 37.8 GHz. Fourn *et al.* [56] then went on to demonstrate another distributed-element RF MEMS filter; cantilever-type capacitive membrane switches were incorporated into the open circuit ends of interdigital CPW resonators. By switching-in an extra section of line, the physical and electrical lengths of the resonators increase, thus, reducing the pass band

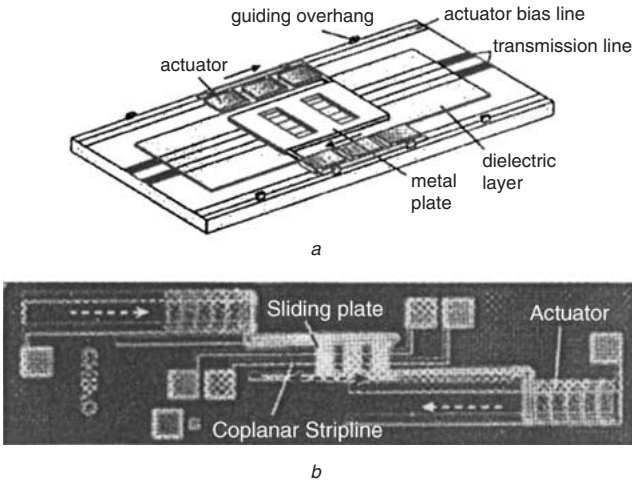

Fig. 8 *Sliding back-short impedance tuner [34]*
a Illustration
b Microphotograph
Reproduced by permission of IEEE

frequency response from 21 GHz down to 19 GHz, with an actuation voltage of 65 V. Having a fused silica substrate, the insertion loss was 4 dB and the return loss was better than 12 dB.

6.3 Signal routing

Signal routing can take many forms; for example, switching between two single-ended HEMT amplifiers, designed to have a different power gain, in order to avoid the drop in power-added efficiency that would occur if digital attenuators were used [57]. In RF subsystems, low loss and high isolation signal routing is very important. When implementing transmitter PA or receiver LNA redundancy subsystems, low loss switching is required to minimise degradation in power-added efficiency and noise performance, respectively. This is also the case when implementing T/R switches within T/R modules and switched-diversity sectorised antennas [58], where very high isolation is also important.

7 Discussion and Conclusions

With the relentless advances in enabling technologies, the RF MEMS foundry services offered to designers will continue to expand. Already, MEMS technology has demonstrated its superiour RF performance over conventional approaches; a raft of new components and circuits has been demonstrated. However, the difficulty in matching the future needs of the RF component designer with the limitations of commercial MEMS foundry processes should not be underestimated. Moreover, there are inherent problems associated with RF MEMS technology. For example, at low microwave frequencies, resonant structures are relatively large and so they can be difficult to move under electromechanical actuation. Also, at millimetre-wave frequencies, resonant structures are relatively small and so the physical discontinuities presented by electromechanical actuators can result in unwanted modeing effects. This goes some way to explain why true RF MEMS antennas have been difficult to implement and why variable inductors have yet to be demonstrated.

There is no overall economic gain in replacing conventional devices with RF MEMS components, however, there may be cost benefits from new architectures that have been enabled with RF MEMS components. At present, mainly within industry, there is intense activity in the areas of RF microsystems reliability and hermetic packaging. The reason for this is that the manufacturing industry is now convinced that RF MEMS technology offers considerable advantages over conventional solutions, even though commercially viable hermetic packaging technologies are only just now being reported [32, 59]. For this reason, it may be a little while longer for RF MEMS technology to be employed in ubiquitous integrated systems.

From the industry's perspective, overall cost is the most important driver, ahead of performance. As a result, it is likely that the switch will continue to be the most important RF MEMS component, with future work investigating its enhanced functionality (e.g. with multiple-pole multiple-throw topologies), subsystem integration (e.g. in signal routing applications) and volume production (e.g. 0.1 to 10 billion switching cycle reliability, hermetic packaging and low cost). The focus of RF MEMS circuits is beginning to change. Digital phase shifters are generally receiving less attention, because they are employed within more specialist applications. However, high-Q tuneable filters are receiving greater attention due to their ubiquitous role in wireless systems. In principle, the air-filled metal-pipe rectangular waveguide can achieve very low transmission losses, making superconducting technologies unnecessary in some applications. If this 3-D guided-wave transmission line can be combined with RF MEMS tuning then a major breakthrough could be achieved in millimetre-wave filter technology. Unfortunately, such technological breakthroughs are unlikely to be demonstrated in the short term and may never become economically viable in the medium-to-long term.

8 Acknowledgment

Work on RF MEMS at Imperial College London, has been partly funded by EPSRC, under Grant no. GR/N06045. This paper was inspired by the European 'Network of Excellence' on Advanced MEMS for RF and Millimeter Wave Communications (AMICOM), FR6-507352, under the 6th Framework Programme of the European Commission. The author also wishes to thank Dr. Rayna Azuma, for helping with the references, Dr. G.W. Dahlmann and Dr. E.M. Yeatman, for supplying Fig. 2, and Dr. Andrew S. Holmes for proof reading this manuscript.

9 References

1 Peterson, K.E.: 'Micromechanical membrane switches on silicon', *IBM J. Res. Dev.*, 1979, **23**, (4), pp. 376–385
2 Lucyszyn, S.: 'Rf MEMS-an introduction'. Proc. Workshop on MEMS for RF and Optoelectronics Applications, part of the Int. Wireless Design Conf., London, UK, May 2002, pp. 3–26
3 Robertson, I.D. and Lucyszyn, S. (Eds.): 'RFIC and MMIC Design and Technology' (IEE, London, 2001)
4 Lucyszyn, S., Budimir, D., Wang, Q.H., and Robertson, I.D.: 'Design of compact monolithic dielectric-filled metal-pipe rectangular waveguides for millimetre-wave applications', *IEE Proc., Microw. Antennas Propag.*, 1996, **143**, (5), pp. 451–453
5 Hirano, M., Nishikawa, K., Toyoda, I., Aoyama, S., Sugitani, S., and Yamasaki, K.: 'Three-dimensional passive circuit technology for ultra-compact MMICs', *IEEE Trans. Microw. Theory Tech.*, 1995, **43**, (12), pp. 2845–2850
6 Toyada, T., Tokumitsu, T., and Aikawa, M.: 'Highly integrated three-dimensional MMIC single-chip receiver and transmitter', *IEEE Trans. Microw. Theory Tech.*, 1996, **44**, (12), pp. 2340–2346
7 Arnold, R.G., and Pedder, D.J.: 'Microwave components in multichip module (MCM-D) technology'. Proc. Microwaves '94 Conf., London, October, 1994, pp. 195–199
8 Kamogawa, K., Tokumitsu, T., and Aikawa, M.: 'Multifrequency microstrip antennas using alumina-ceramic/polyimide multilayer dielectric substrate', *IEEE Trans. Microw. Theory Tech.*, 1996, **44**, (12), pp. 2431–2437
9 Treen, S.A., and Cronin, N.J.: 'Terahertz metal pipe waveguides'. Proc. 18th Int. Conf. on Infrared and Millimetre Waves, London, September, 1993, pp. 470–471

10 Moore, D.F., and Syms, R.R.A.: 'Recent developments in micromachined silicon', *Electron. Commun. Eng. J.*, 1999, **11**(6), pp. 261–270
11 Miao, J., Hartnagel, H.L., Wilson, R.J., and Weiss, B.L.: 'Improved free standing semi-insulating GaAs membranes for sensor applications', *Electron. Lett.*, 1995, **31**(13), pp. 1047–1049
12 Beilenhoff, K., Mutamba, C., Pfeiffer, J., Peerings, J., Simon, A., Lin, C., and Hartnagel, H.L.: 'III-V semiconductor structuring for mm and sub-mm waves'. Presented at Workshop M-FrW3 European Micro-Wave Week, Munich, October, 1999
13 Rutledge, D.B., Schwarz, S.E., Hwang, T.L., Angelakos, D.J., Mei, K.K., and Yokota, S.: 'Antennas and waveguides for far-infrared integrated circuits', *IEEE J. Quantum Electron.*, 1980, **16**, pp. 508–516
14 McGrath, W.R., Walker, C., Yap, M., and Tai, Y-C.: 'Silicon micromachined waveguides for millimeter-wave and submillimeter-wave frequencies', *IEEE Microw. Guid. Wave Lett.*, 1993, **3**, (3), pp. 61–63
15 Harle, L., and Katehi, L.P.B.: 'A vertically integrated micromachined filter', *IEEE Trans. Microw. Theory Tech.*, 2002, **50**, (9), pp. 2063–2068
16 Lubecke, V.M., McGrath, W.R., Stimson, P.A., and Rutledge, D.B.: 'Micromechanical tuning elements in a 620-GHz monolithic integrated circuit', *IEEE Trans. Microw. Theory Tech.*, 1998, **46**, (12), pp. 2098–2103
17 Ribas, R.P., Lescot, J., Leclercq, J.-L., Karam, J.M., and Ndagijimana, F.: 'Micromachined microwave planar spiral inductors and transformers', *IEEE Trans. Microw. Theory Tech.*, 2000, **48**, (8), pp. 1326–35
18 Fan, L., Chen, R.T., Nespola, A., and Wu, M.C.: 'Universal MEMS platforms for passive RF components: suspended inductors and variable capacitors'. Proc. IEEE 11th Annual Int. Workshop on Micro Electromechanical Systems (MEMS), Heidelberg, January, 1998, pp. 29–33
19 Zou, J., Chen, J., and Liu, C.: 'Plastic deformation magnetic assembly (PDMA) of 3D microstructures: technology development and application'. Proc. 11th Int. Conf. on Solid-State Sensors and Actuators, Munich, Germany, June 2001, pp. 1582–1585
20 Lubecke, V.M., Barber, B., Chan, E., Lopez, D., Gross, M.E., and Gammel, P.: 'Self-assembling MEMS variable and fixed RF inductors', *IEEE Trans. Microw. Theory Tech.*, 2001, **49**, (11), pp. 2093–2098
21 Van Shuylenbergh, K., Chua, C.L., Fork, D.K., Lu, J-P., and Griffiths, B.: 'On-chip out-of-place high-Q inductors'. Proc. IEEE Conf. on High Performance Devices, Palo Alto CA, August, 2002, pp. 364–374
22 Dahlmann, G.W., Yeatman, E.M., Young, P.R., Robertson, I.D., and Lucyszyn, S.: 'MEMS high Q microwave inductors using solder surface tension self-assembly'. Proc. IEEE MTT-S Int. Microw. Symp., Phoenix AZ, May, 2001, pp. 329–332
23 Dahlmann, G.W., Yeatman, E.M., Young, P.R., Robertson, I.D., and Lucyszyn, S.: 'High Q achieved in microwave inductors fabricated by parallel self-assembly'. Proc. 11th Int. Conf. on Solid-State Sensors and Actuators (Transducers Eurosensors XV), Munich, Germany, June 2001, pp. 1098–1101
24 Dahlmann, G.W., Yeatman, E.M., Young, P.R., Robertson, I.D., and Lucyszyn, S.: 'Fabrication, RF characteristics and mechanical stability of self-assembled 3D microwave inductors', *Sen. Actuators*, 2002, **97–98**, pp. 215–220
25 Langer, J.-C., Zou, J., Liu, C., and Bernhard, J.T.: 'Micromachined reconfigurable out-of-plane microstrip patch antenna using plastic deformation magnetic actuation', *IEEE Microw. Wirel. Compon. Lett.*, 2003, **13**, (3), pp. 120–122
26 Yeatman, E., Holmes, A., Lucyszyn, S., and Dahlmann, G.: 'Design of a Micro-Electro-Mechanical System (MEMS) RF Technology for a Phase Shifter Suitable for Space Radar Applications'. Final Report, Aug. 2001
27 Rebeiz, G.M., and Muldavin, J.B.: 'RF MEMS switches and switch circuits', *IEEE Microw. Mag.*, 2001, pp. 59–71
28 Goldsmith, C., Lin, T.-H., Powers, B., Wu, W.-R., and Norvell, B.: 'Micromechanical membrane switches for microwave applications', *IEEE MTT-S Int. Microw. Symp. Proc.*, Orlando, FL, May, 1995, pp. 91–94
29 Pacheco, S.P., Katehi, L.P.B., and Nguyen, C.T.-C.: 'Design of low actuation voltage RF MEMS switch', *Proc. IEEE MTT-S Int. Microw. Symp.*, Boston, MA, June, 2000, pp. 165–168
30 Rizk, J., Tan, G-L., Muldavin, J.B., and Rebeiz, G.M.: 'High-isolation W-band MEMS switches', *IEEE Microw. Wirel. Compon. Lett.*, 2001, **11**, (1), pp. 10–12
31 Ruan, M., Tam, G., Vaitkus, R., Wheeler, C., and Shen, J.: 'Micro magnetic latching RF switches'. Proc. Wireless Design Conf., London, May 2002, pp. 59–66
32 Blondy, P., Mercier, D., Cros, D., Guillon, P., Rey, P., Charvet, P., Diem, B., Zanchi, C., Lapierre, L., Sombrin, J., and Quoirin, J.B.: 'Packaged millimetre wave thermal MEMS switch'. Proc. 31st European Microwave Conf., London, September, 2001, pp. 283–286
33 Seeger, J.I., and Crary, S.B.: 'Stabilization of electrostatically actuated mechanical devices'. Proc. IEEE Int. Conf. on Solid-State Sensors and Actuators (Transducers), Chicago, IL, June 1997, pp. 1130–1136
34 Chiao, J.-C., Fu, Y., Choudhury, D., and Lin, L-Y.: 'MEMS millimeterwave components', Proc. IEEE MTT-S Int. Microw. Symp., Anaheim, June, 1999, pp. 463–466
35 Borwick, R.L., Stupar, P.A., DeNatale, J.F., Anderson, R., and Erlandson, R.: 'Variable MEMS capacitors implemented into RF filter systems', *IEEE Trans. Microw. Theory Tech.*, 2003, **51**, (1), pp. 315–319
36 Feng, Z., Zhang, W., Su, B., Harsh, K.F., Gupta, K.C., Bright, V., and Lee, Y.C.: 'Design and modelling of RF MEMS tunable capacitors using electro-thermal actuators', Proc. IEEE MTT-S Int. Microw. Symp., Anaheim, June, 1999, pp. 1507–1510
37 Chiao, J.-C., Fu, Y., Chio, I.M., Delisio, M., and Lin, L.Y.: 'MEMS reconfigurable Vee antenna', IEEE MTT-S Int. Microw. Symp., Anahein, June, 1999, pp. 1515–1518
38 Baek, C.-W., Song, S., Park, J.-H., Lee, S., Kim, J.-M., Choi, W., Cheon, C., Kim, Y.-K., and Kwon, Y.: 'A V-band micromachined 2-D beam-steering antenna driven by magnetic force with polymer-based hinges', *IEEE Trans. Microw. Theory Tech.*, 2003, **51**, (1), pp. 325–331
39 Pillans, B., Eshelman, S., Malczewski, A., Ehmke, J., and Goldsmith, C.: 'Ka-band RF MEMS phase shifters', *IEEE Microw. Guid. Wave Lett.*, 1999, **9**, (12), pp. 520–522
40 Kim, M., Mihailovich, R.E., and DeNatale, J. F.: 'A DC-to-40 GHz four-bit RF MEMS true-time delay network', *IEEE Microw. Wirel. Compon. Lett.*, 2001, **11**, (2), pp. 56–58
41 Hacker, J.B., Mihailovich, R.E., Kim, M., and DeNatale, J.F.: 'A Ka-band 3-bit RF MEMS true-time-delay network', *IEEE Trans. Microw. Theory Tech.*, 2003, **51**, (1), pp. 305–308
42 Tan, G.-L., Mihailovich, R.E., Hacker, J.B., DeNatale, J.F., and Rebeiz, G.M.: 'Low-loss 2- and 4-bit TTD MEMS phase shifters based on SP4T switches', *IEEE Trans. Microw. Theory Tech.*, 2003, **51**, (1), pp. 297–304
43 Malczewski, A., Eshelman, S., Pillans, B., Ehmke, J., and Goldsmith, C.L.: 'X-band RF MEMS phase shifters for phased array applications', *IEEE Microw. Guid. Wave Lett.*, 1999, **9**, (12), pp. 517–519
44 Borgioli, A., Liu, Y., Nagra, A.S., and York, R.A.: 'Low-loss distributed MEMS phase shifter', *IEEE Microw. Guid. Wave Lett.*, 2000, **10**, (1), pp. 7–9
45 Liu, Y., Borgioli, A., Nagra, A.S., and York, R.A.: 'K-band 3-bit low-loss distributed MEMS phase shifter', *IEEE Microw. Guid. Wave Lett.*, 2000, **10**, (10), pp. 415–417
46 Hayden, J.S., and Rebeiz, G.M.: 'Low-loss cascadable MEMS distributed X-band phase shifters', *IEEE Microw. Guid. Wave Lett.*, 2000, **10**, (4), pp. 142–144
47 Hayden, J.S., and Rebeiz, G.M.: '2-bit MEMS distributed X-band phase shifters', *IEEE Microw. Guid. Wave Lett.*, 2000, **10**, (12), pp. 540–542
48 Kim, H.-K., Park, J.-H., Lee, S., Kim, S., Kim, J.-M., Kim, Y.-K., and Kwon, Y.: 'V-band 2-b and 4-b low-loss and low-voltage distributed MEMS digital phase shifter using metal-air-metal capacitors', *IEEE Trans. Microw. Theory Tech.*, 2002, **50**, (12), pp. 2918–2923
49 Hayden, J.S., and Rebeiz, G.M.: 'Very low-loss distributed *X*-band and Ka-band MEMS phase shifters using metal-air-metal capacitors', *IEEE Trans. Microw. Theory Tech.*, 2003, **51**, (1), pp. 309–314
50 Kim, H.-K., Jung, S., Kang, K., Park, J.-H., and Kim, Y.-K.: 'Low-loss analog and digital micromachined impedance tuners at the Ka-band', *IEEE Trans. Microw. Theory Tech.*, 2001, **49**, (12), pp. 2394–2400
51 Papapolymerou, J., Lange, K.L., Goldsmith, C.L., Malczewski, A., and Kleber, J.: 'Reconfigurable double-stub tuners using MEMS switches for intelligent RF front-ends', *IEEE Trans. Microw. Theory Tech.*, 2003, **51**, (1), pp. 271–278
52 Seok, S., Nam, C., Choi, W., Choi, S.D., and Chun, K.: 'A novel MEMS LC tank for RF voltage controlled oscillator (VCO)'. Paper 4C1.05P, Proc. 11th Int. Conf. on Solid-State Sensors and Actuators (Transducers Eurosensors XV), Munich, June 2001, pp. 1544–1547
53 Kim, H-K., PARK, J-H., Kim, Y-K., and Kwon, Y.: 'Millimeter-wave micromachined tunable filters', *Proc. IEEE MTT-S Int. Microw. Symp.*, Anahein, June, 1999, pp. 1235–1238
54 Kim, H-K., Park, J-H., Kim, Y-K., and Kwon, Y.: 'Low-loss and compact V-band MEMS-based analog tunable bandpass filters', *IEEE Microw. Wirel. Compon. Lett.*, 2002, **12**, (11), pp. 432–434
55 Mercier, D., Blondy, P., Cros, D., and Guillon, P.: 'Distributed MEMS tunable filters'. Proc. 31st European Microwave Conf., London, September, 2001, pp. 9–12
56 Fourn, E., Pothier, A., Champeaux, C., Tristant, P., Catherinot, A., Blondy, P., Tanné, G., Rius, E., Person, C., and Huret, F.: 'MEMS switchable interdigital coplanar filter', *IEEE Trans. Microw. Theory Tech.*, 2003, **51**, (1), pp. 320–324
57 Kim, M., Hacker, J.B., Mihailovich, R.A., and DeNatale, J.F.: 'A monolithic MEMS switched dual-path power amplifier', *IEEE Microw. Wirel. Compon. Lett.*, 2001, **11**, (7), pp. 285–286
58 Cetiner, B.A., Qian, J.Y., Chang, H.P., Bachman, M., Li, G.P., and De Flaviis, F.: 'Monolithic integration of RF MEMS switches with a diversity antenna on PCB substrate', *IEEE Trans. Microw. Theory Tech.*, 2003, **51**, (1), pp. 332–335
59 Varian, K., and Walton, D.: 'A 2-bit RF MEMS phase shifter in a thick-film BGA ceramic package', *IEEE Trans. Microw. Theory Tech.*, 2002, **12**, (9), pp. 321–323